J. Fluid Mech. (1984), *vol.* 138, *pp.* 75–91
Printed in Great Britain

Scalar diffusion in simulated helical turbulence with molecular diffusivity

By I. T. DRUMMOND, S. DUANE AND R. R. HORGAN
Department of Applied Mathematics and Theoretical Physics, University of Cambridge, Silver Street, Cambridge CB3 9EW

(Received 28 April 1983)

We extend the simulation techniques of Kraichnan (1970, 1976) to study the effective diffusivity of a scalar field in a turbulent fluid. In our model we have introduced an adjustable helicity parameter and a technique for simulating molecular diffusivity. The results show that for non-helical turbulence the self-consistent perturbation theory of Phythian & Curtis (1978) gives excellent values for the effective diffusivity over a wide range of values for both the molecular diffusivity and the parameters describing the turbulence.

This ceases to be the case immediately the helicity is given a non-zero value. Wide departures are observed between the theoretical calculation and the simulation. Our conclusion is that non-perturbative effects are very important in the presence of helicity.

1. Introduction

In this paper we report on a numerical simulation of the time evolution in three dimensions of a scalar field subject to molecular diffusion and convection in a turbulent fluid. The problem of calculating the time evolution of a scalar field under such conditions is a long-standing one. We investigate the short- and long-time behaviour of the evolution in some particular cases and compare the results with theoretical calculations, paying particular attention to the comparison between the long-time effective diffusivity measured in the simulation and predicted in the self-consistent perturbation series of Phythian & Curtis (1978), in all cases a variable helicity is present in the turbulence and the dependence of measured quantities on the parameter controlling the helicity is carefully examined.

Our simulation is an extension of the original studies of Kraichnan (1970, 1976, 1977). The new features that we have included are (i) the adjustable helicity for the turbulent flow and (ii) a molecular diffusivity for the fluid. We have implemented a new algorithm for the simulation which allows the molecular diffusivity to be introduced. Our ability to vary both the helicity and the molecular diffusivity proved to be extremely useful and provided revealing results.

The turbulence was represented by an incompressible random velocity field which was chosen from a Gaussian distribution. For simplicity the autocorrelation function of the velocity ensemble was chosen to be of a simple kind (to facilitate the theoretical calculation) and was characterized by only one length- and one timescale. However, the simulation does not depend for its success on this choice of spectrum for the turbulence or on the precise number of relevant space–time scales.

All computing was carried out on the ICL Distributed Array Processor (DAP) at

Queen Mary College, London, and we were able to exploit the potential of the DAP for producing large numbers of statistics to obtain good numerical results in a reasonable computation time.

In §2 we show how the velocity field is constructed for a given autocorrelation function. The way in which we introduce an adjustable helicity is explained, and the particular autocorrelation function used in our simulation is presented. In §3 the numerical-integration procedure is discussed and we present our algorithm for evolving the scalar field subject to diffusion and convection by the turbulent fluid. In §4 the simulation on the DAP and the calculation of errors are discussed. We present the results of the simulation and the comparison with theory in §§5 and 6. The results for the short-time behaviour are discussed in §5 for various values of the parameters. The results for the long-time behaviour are given in §6, where the dependence of the effective diffusivity on the molecular diffusivity and the helicity is presented and compared with theory. In §7 we present our conclusions.

2. The velocity-field ensemble

Following Kraichnan (1970, 1976) we generate the velocity field $\boldsymbol{u}(\boldsymbol{x}, t)$ as a sum of Fourier components, each of which is determined by certain parameters distributed according to various probability distributions. The number N of terms in the sum is sufficiently large so that an ensemble of velocity fields is Gaussian in character up to corrections of order $1/N$. In this case all higher correlation functions are determined by the autocorrelation function

$$\langle u_i(\boldsymbol{x}, t)\, u_j(\boldsymbol{x}', t')\rangle = \int \frac{\mathrm{d}^3k\, \mathrm{d}\omega}{(2\pi)^3} \mathrm{e}^{\mathrm{i}\boldsymbol{k}\cdot(\boldsymbol{x}-\boldsymbol{x}')+\mathrm{i}\omega(t-t')} F_{ij}(\boldsymbol{k}, \omega). \tag{2.1}$$

We have assumed that the ensemble is homogeneous, and we also assume that it is isotropic, in which case, for incompressible fluids, we have

$$F_{ij}(k, \omega) = \Phi(k, \omega)\,(k^2\delta_{ij} - k_i k_j) + \Psi(k, \omega)\,\mathrm{i}\epsilon_{imj} k_m, \tag{2.2}$$

where $\Psi(k, \omega)$ represents the presence of helicity.

A particular member of the velocity-field ensemble is then realized by

$$\begin{aligned}\boldsymbol{u}(\boldsymbol{x}, t) = A \sum_{n=1}^{N} \{&(\boldsymbol{\xi}_n \cos\psi_n - \boldsymbol{\chi}_n \times \hat{\boldsymbol{k}}_n \sin\psi_n) \times \boldsymbol{k}_n \cos(\boldsymbol{k}_n \cdot \boldsymbol{x} + \omega_n t) \\ &+ (\boldsymbol{\chi}_n \cos\psi_n + \boldsymbol{\xi}_n \times \hat{\boldsymbol{k}}_n \sin\psi_n) \times \boldsymbol{k}_n \sin(\boldsymbol{k}_n \cdot \boldsymbol{x} + \omega_n t)\}.\end{aligned} \tag{2.3}$$

This is more elaborate than either of the forms used by Kraichnan (1970, 1976), but the presence of the angle ψ_n allows us to introduce an adjustable amount of helicity into the turbulence. The random variables $(\boldsymbol{\xi}_n, \boldsymbol{\chi}_n, \boldsymbol{k}_n, \omega_n)$ are chosen in the following way.

The vectors $\boldsymbol{\xi}_n$ and $\boldsymbol{\chi}_n$ are distributed uniformly and independently over the unit sphere. The wavenumber $\boldsymbol{k}_n$ and the frequency variable are independently distributed according to a probability distribution $P(\boldsymbol{k}, \omega)$, which in practice is taken to have the factorized form $E(k^2)\, D(\omega)$. In what follows the angle variable ψ_n is set equal to a given value ψ (for all n), which we call the helicity parameter. It is sufficient that $|\psi| \leqslant \frac{1}{4}\pi$. The overall normalization of the velocity field A is determined by the value for the r.m.s. velocity $\boldsymbol{u}_0$.

If h and Ω denote the helicity and r.m.s. vorticity respectively then

$$\left.\begin{aligned} u_0^2 &= \langle \boldsymbol{u}\cdot\boldsymbol{u}\rangle = \tfrac{2}{3}A^2\left\langle \sum_{n=1}^{N} k_n^2 \right\rangle = \tfrac{2}{3}A^2 N\int \mathrm{d}^3k\, E(k^2)\, k^2, \\ h &= \langle \boldsymbol{u}\cdot(\boldsymbol{\nabla}\times\boldsymbol{u})\rangle = \tfrac{2}{3}A^2\left\langle \sum_{n=1}^{N} k_n^3 \sin 2\psi_n \right\rangle \\ &= \tfrac{2}{3}A^2 N\int \mathrm{d}^3k\, E(k^2)\, k^3 \sin 2\psi(k), \\ \Omega^2 &= \langle(\boldsymbol{\nabla}\times\boldsymbol{u})^2\rangle = \tfrac{2}{3}A^2\left\langle \sum_{n=1}^{N} k_n^4 \right\rangle = \tfrac{2}{3}A^2 N\int \mathrm{d}^3k\, E(k^2)\, k^4. \end{aligned}\right\} \tag{2.4}$$

The last equality in each line holds for N sufficiently large.

Because we restrict ourselves to a constant helicity parameter ψ, Φ and Ψ in (2.2) are both simply related to $E(k^2)$. We find

$$\left.\begin{aligned} \Phi(k,\omega) &= \tfrac{1}{3}(2\pi)^3 A^2 N E(k^2)\, D(\omega), \\ \Psi(k,\omega) &= \tfrac{1}{3}(2\pi)^3 A^2 N E(k^2)\, kD(\omega)\sin 2\psi. \end{aligned}\right\} \tag{2.5}$$

In our model then

$$\Psi(k,\omega) = \Phi(k,\omega)\, k\sin 2\psi. \tag{2.6}$$

In order to keep the problem of simulation as simple as possible we consider the case of one-scale turbulence. These are the same circumstances as investigated by Kraichnan (1970, 1976, 1977). Furthermore, because it makes the theoretical analysis a little easier, we will work with a δ-shell for $E(k^2)$, thus

$$E(k) = \frac{1}{4\pi k_0^2}\delta(k-k_0), \tag{2.7}$$

where k_0 is the characteristic wavenumber of the turbulence. For the frequency distribution we choose

$$D(\omega) = \frac{1}{(2\pi)^{\frac{1}{2}}\omega_0}\mathrm{e}^{-\frac{1}{2}\omega^2/\omega_0^2}. \tag{2.8}$$

We then find

$$\left.\begin{aligned} A &= \left(\frac{3}{2N}\right)^{\frac{1}{2}}\frac{u_0}{k_0}, \\ h &= u_0^2 k_0 \sin 2\psi, \\ \Omega^2 &= u_0^2 k_0^2, \end{aligned}\right\} \tag{2.9}$$

and

$$\langle \boldsymbol{u}(\boldsymbol{x},t)\cdot\boldsymbol{u}(\boldsymbol{x}',t')\rangle = u_0^2\frac{\sin k_0 r}{k_0 r}\mathrm{e}^{-\frac{1}{2}\omega_0^2(t-t')^2}, \tag{2.10}$$

where $r = |\boldsymbol{x}-\boldsymbol{x}'|$.

We also have

$$\langle \boldsymbol{\omega}(\boldsymbol{x},t)\cdot\boldsymbol{u}(\boldsymbol{x}',t')\rangle = k_0\sin 2\psi\langle \boldsymbol{u}(\boldsymbol{x},t)\cdot\boldsymbol{u}(\boldsymbol{x}',t')\rangle, \tag{2.11}$$

where $\boldsymbol{\omega}(\boldsymbol{x},t)$ is the vorticity given by $\boldsymbol{\omega} = \boldsymbol{\nabla}\times\boldsymbol{u}$.

Although our spectrum is unrealistically simple the results obtained are nevertheless significant. More-complicated spectra with more than one scale in the turbulence are of greater interest, but require more computing effort in the simulation. We restrict our attention to the simplest case for the present.

As an indication of how well the simulation reproduces the correlation function we

calculated the ratio of the simulated functions to the analytic forms in equations (2.10) and (2.11) for various values of the parameters. Over a range of over three correlation lengths and one correlation time these ratios were unity within statistical errors, which were typically less than 1%.

A more stringent test of the simulated ensemble concerns its Gaussian character. Assuming Gaussianity, we expect to find that

$$\langle \boldsymbol{u}^2(\boldsymbol{x},t)\,\boldsymbol{u}(\boldsymbol{x},t)\cdot\boldsymbol{u}(\boldsymbol{x}',t')\rangle = \tfrac{5}{3}u_0^2\langle \boldsymbol{u}(\boldsymbol{x},t)\cdot\boldsymbol{u}(\boldsymbol{x}',t')\rangle. \tag{2.12}$$

A comparison of the computed value of the left-hand side to the computed value of the right-hand side for $N = 64$ (see (2.3)) in the case $k_0 = 6$, $\omega_0 = 1$, $\psi = 0$ showed that this equation is satisfied within statistical errors (in 1%). This agreement was checked over more than three correlation lengths in space and one in time. We expect deviations to be of order $1/N$, and this expectation is verified. For reasonable values of N any departure from Gaussianity is certainly negligible.

3. Numerical-integration procedure

In the absence of molecular diffusivity the problem of following a particle path in a velocity field $\boldsymbol{u}(\boldsymbol{x},t)$ is solved by integrating, to sufficient accuracy, the differential equation

$$\dot{\boldsymbol{x}} = \boldsymbol{u}(\boldsymbol{x},t). \tag{3.1}$$

When molecular diffusivity κ is present we must deal with the stochastic differential equation

$$\dot{\boldsymbol{x}} = \boldsymbol{u}(\boldsymbol{x},t)+\boldsymbol{\eta}(t), \tag{3.2a}$$

the discrete version of which is

$$\Delta\boldsymbol{x} = \boldsymbol{u}(\boldsymbol{x},t)\,\Delta t+(2\kappa\Delta t)^{\frac{1}{2}}\boldsymbol{\xi}. \tag{3.2b}$$

Here $\boldsymbol{\eta}(t)$ is a Gaussian random variable with zero mean and autocorrelation function $\langle \boldsymbol{\eta}(t)\cdot\boldsymbol{\eta}(t')\rangle = 2\kappa\delta(t-t')$. The quantity $\boldsymbol{\xi}$ is a Gaussian random variable of zero mean and unit variance. It is well known that for infinitesimally small Δt the resulting probability distribution $\phi(\boldsymbol{x},t)$ of the particle position $\boldsymbol{x}$ satisfies the diffusion equation

$$\frac{\partial\phi}{\partial t}+\boldsymbol{\nabla}\cdot(\boldsymbol{u}\phi) = \kappa\nabla^2\phi. \tag{3.3}$$

If (3.2*b*) is used to increment the particle position, then for finite Δt there are corrections to (3.3) or order Δt. In order to increase the accuracy of the method most efficiently it is advantageous to use a modified form of (3.2*b*) which eliminates errors up to a specified order in Δt. A modification of this kind is discussed in Drummond, Duane & Horgan (1983), where the elimination of the $O(\Delta t)$ errors is achieved by the prescription

$$\Delta\boldsymbol{x} = \left[\boldsymbol{u}(\boldsymbol{x},t)+\tfrac{1}{2}\Delta t\left(\boldsymbol{u}\cdot\boldsymbol{\nabla}+\frac{\partial}{\partial t}\right)\boldsymbol{u}(\boldsymbol{x},t)+\tfrac{1}{2}\Delta t\kappa\nabla^2\boldsymbol{u}(\boldsymbol{x},t)\right]\Delta t+(2\kappa\Delta t)^{\frac{1}{2}}\boldsymbol{\xi}, \tag{3.4}$$

where $\boldsymbol{\xi}$ is normally distributed about zero with a variance matrix

$$\langle \xi_i\xi_j\rangle = \delta_{ij}+\tfrac{1}{2}(u_{i,j}+u_{j,i})\,\Delta t. \tag{3.5}$$

It is in fact more convenient to adopt a slightly different prescription which differs from (3.4) only in irrelevant orders of Δt. This prescription takes the form of an extended Runge–Kutta scheme:

$$\Delta\boldsymbol{x} = \boldsymbol{u}(\boldsymbol{x}',t)\,\Delta t+(\kappa\Delta t)^{\frac{1}{2}}(\boldsymbol{\xi}_1+\boldsymbol{\xi}_2), \tag{3.6}$$

where
$$\left.\begin{aligned} t' &= t+\tfrac{1}{2}\Delta t, \\ \boldsymbol{x}' &= \boldsymbol{x}+\tfrac{1}{2}\Delta t\,\boldsymbol{u}(\boldsymbol{x},t)+(\kappa\Delta t)^{\frac{1}{2}}\boldsymbol{\xi}_1. \end{aligned}\right\} \tag{3.7}$$

$\boldsymbol{\xi}_1$ and $\boldsymbol{\xi}_2$ are independent random variables each with zero mean and unit variance.

The superiority of the extended Runge–Kutta scheme over the scheme of (3.4) is that in the former case no derivatives of the velocity field need be calculated. The saving in computation time is significant: the time required by an nth-order Runge–Kutta scheme only rises like n. Higher-order schemes of the kind shown in (3.4) require times that increase probably like $n!$.

We use a third-order Runge–Kutta scheme, which is described in the appendix. We note, however, that, although efficient, this scheme minimizes the error at $O(\Delta t)^3$ rather than reducing it to $O(\Delta t^4)$.

For zero diffusivity when (3.1) is appropriate we also implemented a fourth-order predictor–corrector scheme of the kind used by Kraichnan. In this case the results of this method did not differ significantly from the results of the Runge–Kutta scheme.

4. The simulation

The DAP is a 64×64 array of microprocessors acting in parallel. In realizing the simulation of the turbulent fluid outlined above, it was convenient therefore to use a velocity field with $N = 64$ components. Other values of N were also studied for the purposes of comparison.

In a typical cycle of calculation the machine contained 64 different velocity fields, each with 64 different particles, the starting points of which were separated by two velocity correlation lengths. The histories of these 4096 particles were followed simultaneously for any desired number of time steps with an appropriately chosen Δt smaller than the smallest timescale characterizing the turbulence. This cycle was repeated as many times as was feasible in order to reduce the statistical errors. In a typical run the number of cycles was 25; thus the flow of 102400 particles in 1600 velocity fields was investigated. The average of relevant quantities over the ensemble of paths so generated was computed. In order to estimate the statistical error on these averages a mini-ensemble of estimators for a particular averaged quantity (g say) was constructed. Each member $\langle g\rangle_{(i)}$ of the mini-ensemble was the average value of g taken over the paths of one velocity field $\boldsymbol{u}_{(i)}$. The members of the mini-ensemble were statistically independent because the velocity fields were. The error σ on a final estimator $\langle g\rangle$ for g is computed by the usual methods from the mini-ensemble:

$$\left.\begin{aligned} \langle g\rangle &= \frac{1}{M}\sum_{i=1}^{M}\langle g\rangle_{(i)}, \\ \sigma^2 &= \frac{1}{M(M-1)}\sum_{i=1}^{M}(\langle g\rangle_{(i)}^2-\langle g\rangle^2). \end{aligned}\right\} \tag{4.1}$$

It is interesting to note that a calculation of σ that treats *all* particles as being statistically independent of each other leads to a value very similar to that obtained by the method outlined above. This is important because it demonstrates that all the particles moving in one velocity field are substantially uncorrelated and hence make a maximum contribution to the reduction of errors. Consequently we are not wasting computing effort by duplicating particle flows.

5. Short-time evolution

We are interested ultimately in the long-time evolution of the particle distribution. However, the dispersion at long times is the accumulated result of many processes occurring over short time intervals. In order to have confidence in the results of the simulation and the integration procedure it is important to check that the evolution of averaged quantities (e.g. $\langle \boldsymbol{x}^2(t)\rangle$ and $\langle (\boldsymbol{x}^2(t))^2\rangle$) over short times is correctly reproduced by our numerical techniques.

For an appropriately short time interval those quantities may be expressed as Taylor series in the time t. In the case of homogeneous turbulence without molecular diffusivity we have

$$\langle \boldsymbol{x}^2\rangle = \langle \boldsymbol{u}^2\rangle t^2 - \tfrac{1}{12}\langle \mathrm{D}\boldsymbol{u}\cdot \mathrm{D}\boldsymbol{u}\rangle + \tfrac{1}{360}\langle \mathrm{D}^2\boldsymbol{u}\cdot \mathrm{D}^2\boldsymbol{u}\rangle t^6 + O(t^8), \tag{5.1}$$

where $\mathrm{D} = \partial/\partial t + \boldsymbol{u}\cdot\nabla$ is the material time derivative, and all correlations are at equal times and positions. If we use the spectrum described in §2, (2.7)–(2.11), and use the assumed isotropic and Gaussian nature of the turbulence, we find

$$\begin{aligned}\langle \boldsymbol{x}^2(t)\rangle - u_0^2 t^2 = {} & -\tfrac{1}{12}(\omega_0^2 u_0^2 + \tfrac{1}{3}u_0^4 k_0^2(1-\tfrac{1}{2}x^2))\, t^4 \\ & + \tfrac{1}{360}(3\omega_0^4 u_0^2 + \omega_0^2 u_0^4 k_0^2(\tfrac{7}{3}-x^2) + u_0^6 k_0^4(\tfrac{2}{5}-\tfrac{1}{4}x^2))\, t^6 + O(t^8) \equiv Y_2(t), \end{aligned} \tag{5.2}$$

where $x = \sin 2\psi$. We have also

$$\langle (\boldsymbol{x}^2(t))^2\rangle - \tfrac{5}{3}u_0^4 t^4 = -\tfrac{5}{18}(\omega_0^2 u_0^4 + u_0^6 k_0^2(\tfrac{7}{15}-\tfrac{1}{6}x^2))\, t^6 + O(t^8) \equiv Y_4(t). \tag{5.3}$$

It is important to recognize that these equations are only strictly correct in the limit of infinite statistics and large N. In practice these equations give the predicted value of some required mean, which is to be compared with a random number which is the estimator for that mean. For this comparison to be significant we require that the error on the estimator is much smaller than the magnitude of the signal that we are seeking. In order to test the higher-order terms in the short-time perturbation theory this error must be much smaller than the terms on the right-hand sides of (5.2) and (5.3) (denoted by $Y_2(t)$ and $Y_4(t)$ respectively). In order to achieve this most efficiently it is useful to take advantage of the cancellation of errors which may occur when quantities are measured over the same ensemble. We introduce statistical variables $X_2(t)$ and $X_4(t)$, the mean values of which, in a perfect ensemble, reduce to the left-hand sides of (5.2) and (5.3) respectively. These variables are given by

$$X_2(t) = \boldsymbol{x}^2(t) - t\Delta t \sum_{r=0}^{n-1} \boldsymbol{u}^2(\boldsymbol{x}_r, t_r), \tag{5.4}$$

$$X_4(t) = (\boldsymbol{x}^2(t))^2 - t^3\Delta t \sum_{r=0}^{n-1} (\boldsymbol{u}^2(\boldsymbol{x}_r, t_r))^2, \tag{5.5}$$

where $\boldsymbol{x}_n = \boldsymbol{x}$, $t_n = t$, and $(\boldsymbol{x}_r, t_r)$ is the position and time of the particle after r steps. The size of the time step is Δt.

Of course any choice of estimators is suitable provided they are Gaussian random variables whose means are predictable using (5.2) and (5.3) respectively. Note that the ratio $R = \langle (\boldsymbol{x}^2(t))^2\rangle / \langle \boldsymbol{x}^2(t)\rangle^2$ is not a suitable estimator even though the predicted value is simple. Our choice is justified because it works well.

In figures 1 and 2 we plot the ratios

$$R_2(t) = \frac{\langle X_2(t)\rangle}{Y_2(t)}, \quad R_4(t) = \frac{\langle X_4(t)\rangle}{Y_4(t)} \tag{5.6}$$

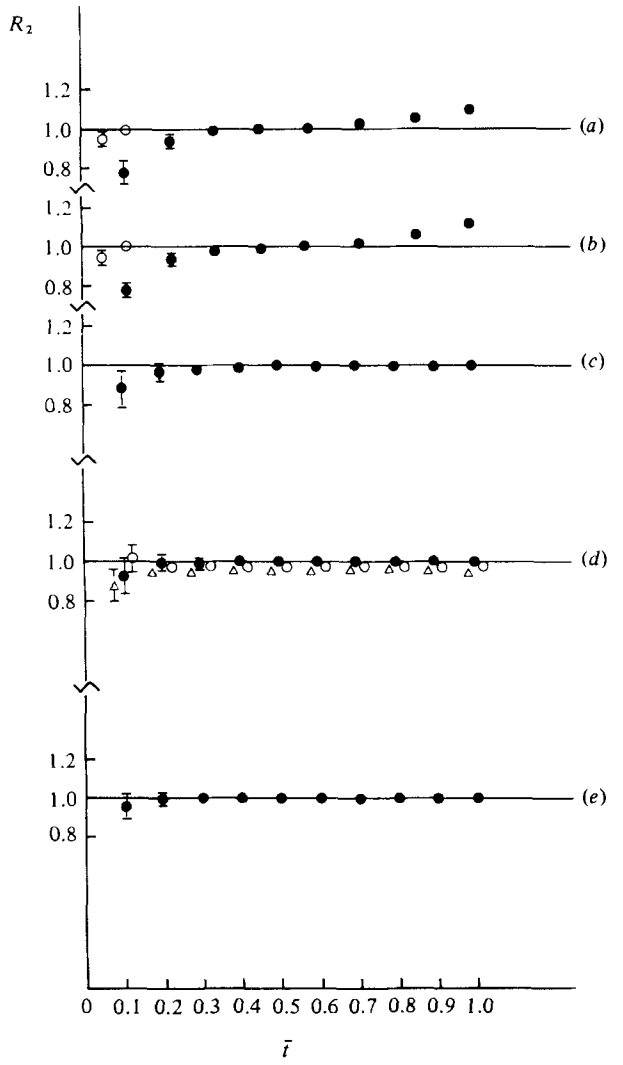

FIGURE 1. The ratio $R_2 = \langle X_2(t)\rangle / Y_2(t)$, with $Y_2(t)$ given by theory in (5.2) and $X_2(t)$ defined by (5.4). The time axis is scaled as follows: (*a*) $k_0 = 1$, $\omega_0 = 6$, $x^2 = 0$, $t = \sqrt{3}\,\bar{t}/\omega_0$; (*b*)1, 3, 0, $\sqrt{3}\,\bar{t}/\omega_0$; (*c*), 6, 1, 1.0, $\bar{t}/k_0$; (*d*) 6, 1, 0.5, $\bar{t}/k_0$; (*e*) 6, 1, 0, $\bar{t}/k_0$. The helicity parameter is $x = \sin 2\psi$. The integration time step Δt is 0.02 (●) or 0.004 (○). For case (*d*) results are shown for different numbers N of components in the velocity field: ●, 64; ○, 32; △, 16. Otherwise all results are for $N = 64$.

against t for times small compared with any characteristic period of the turbulence, i.e. $\Omega t, \omega_0 t < 1$ (see §2). Various values of the helicity, k_0, and ω_0 are chosen. The ratio $R_2(t)$ is very close to unity in all cases, except for an inevitable discrepancy at extremely short times due to the finite step length of the integration procedure.

For short times $R_4(t)$ is unity, and the deviation for larger times is compatible with the correction term in (5.3), which behaves like t^8. Unfortunately this term is very hard to calculate and so has not been included. Originally the $O(t^6)$ term was omitted from (5.2) and a similar discrepancy was found in $R_2(t)$, which was corrected by the subsequent inclusion of this term. Since these results depend heavily on the assumption of Gaussianity and on the effectiveness of the integration procedure, the

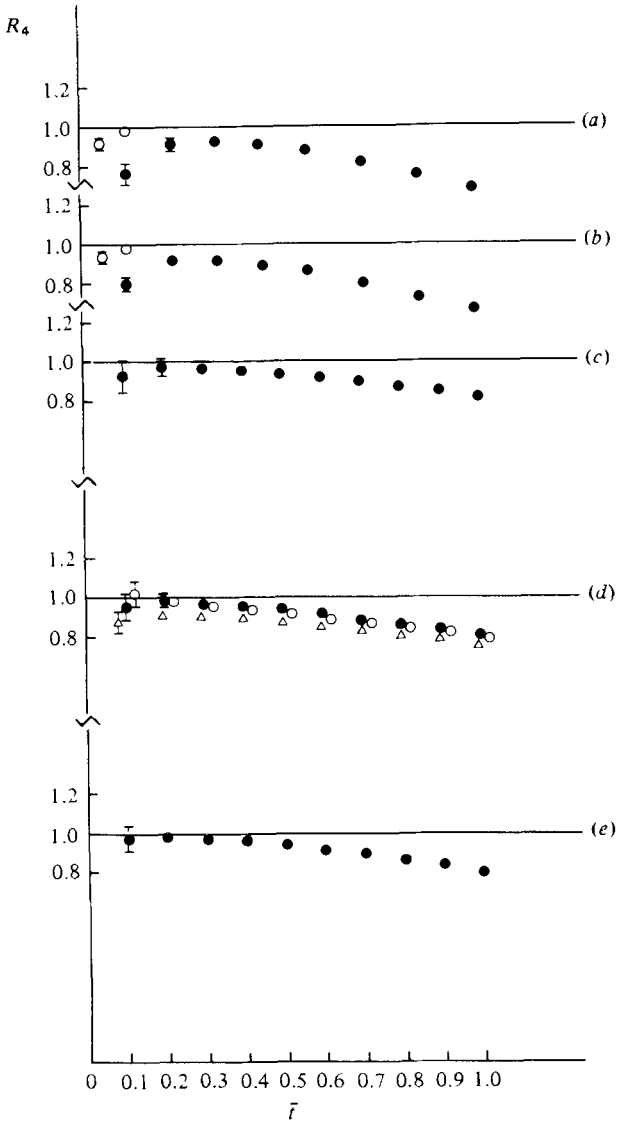

FIGURE 2. As figure 1 for the ratio $R_4 = \langle X_4(t)\rangle / Y_4(t)$, with $Y_4(t)$ given in (5.3) and $X_4(t)$ defined by (5.5).

success of the comparison is strong support for both aspects of the simulation. The error bars are calculated in the way described in §4. That the errors are so small indicates that the accumulated statistics are sufficient.

When molecular diffusivity is introduced we find

$$\langle \boldsymbol{x}(t)^2\rangle - 6\kappa t - u_0^2 t^2 = -\tfrac{1}{3}\kappa u_0^2 k_0^2 t^3 + \tfrac{1}{12}u_0^2[\kappa^2 k_0^4 - \omega_0^2 - \tfrac{1}{3}u_0^2 k_0^2(1-\tfrac{1}{2}x^2)]\, t^4$$
$$-\tfrac{1}{120}[\kappa^3 k_0^6 + 3\omega_0^2 \kappa k_0^2]\, u_0^2 t^5 + O(t^6) \equiv Y_2'(t), \quad (5.7)$$

$$\langle (\boldsymbol{x}(t)^2)^2\rangle - 60\kappa^2 t^2 - \tfrac{5}{3}u_0^4 t^4 = 20\kappa u_0^2 t^3 - 8\kappa^2 u_0^2 k_0^2 t^4 + [\tfrac{37}{15}\kappa^3 k_0^4 - \tfrac{5}{3}\kappa\omega_0^2]\, u_0^2 t^5$$
$$-[\tfrac{3}{5}\kappa^4 k_0^6 - \tfrac{19}{15}\kappa^2 k_0^2 \omega_0^2 + \tfrac{5}{18}u_0^2(\omega_0^2 + \tfrac{7}{15}u_0^2 k_0^2(1-\tfrac{5}{14}x^2))]\, u_0^2 t^6 + O(t^7) \equiv Y_4'(t). \quad (5.8)$$

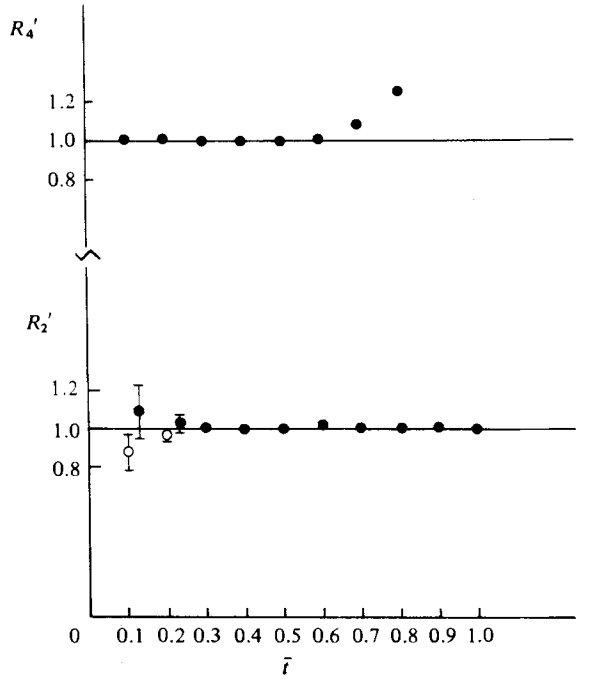

FIGURE 3. The ratios $R_2' = \langle X_2'(t)\rangle / Y_2'(t)$ and $R_4' = \langle X_4'(t)\rangle / Y_4'(t)$, with Y_2' and Y_4' defined in (5.7) and (5.8) respectively, and X_2' and X_4' defined respectively by (5.9) and (5.10). The curves are for $k_0 = 6$, $\omega_0 = 0$, $\kappa = 0.5$.

This formula omits certain terms $O(u_0^4)$ such as $\kappa^2 u_0^4 k_0^4 t^6$, mainly because they are difficult to calculate. It is plausible for our choice of parameters that they are small and the numerical results bear this out.

Note that the first term on the right-hand side of (5.7) is the term obtained by Saffman (1960) which shows the negative interaction of vorticity and diffusivity. As before we use specially chosen statistical variables to test (5.7) and (5.8), namely

$$X_2'(t) = X_2(t) - \langle \boldsymbol{x}_0^2(t)\rangle, \tag{5.9}$$

$$X_4'(t) = X_4(t) - \langle (\boldsymbol{x}_0^2(t))^2\rangle, \tag{5.10}$$

where $\boldsymbol{x}_0(t)$ is the path followed by an auxiliary particle for which there is no turbulent transport ($u_0 = 0$) but which diffuses using the *same* random numbers and integration procedure as the particle with which it is associated.

The ratios

$$R_2'(t) = \frac{\langle X_2'(t)\rangle}{Y_2'(t)}, \quad R_4'(t) = \frac{\langle X_4'(t)\rangle}{Y_4'(t)} \tag{5.11}$$

are plotted against time in figure 3 for various values of the parameters. Again the agreement with theoretical prediction is so good that we can be confident that the numerical procedures of the simulation are working extremely well.

6. Long-time behaviour

Kraichnan (1970, 1976, 1977) in his computer studies of turbulent diffusion confirmed the idea that at large times the dispersion of particles increases linearly with time and that there is an asymptotic diffusivity. Our calculations are entirely

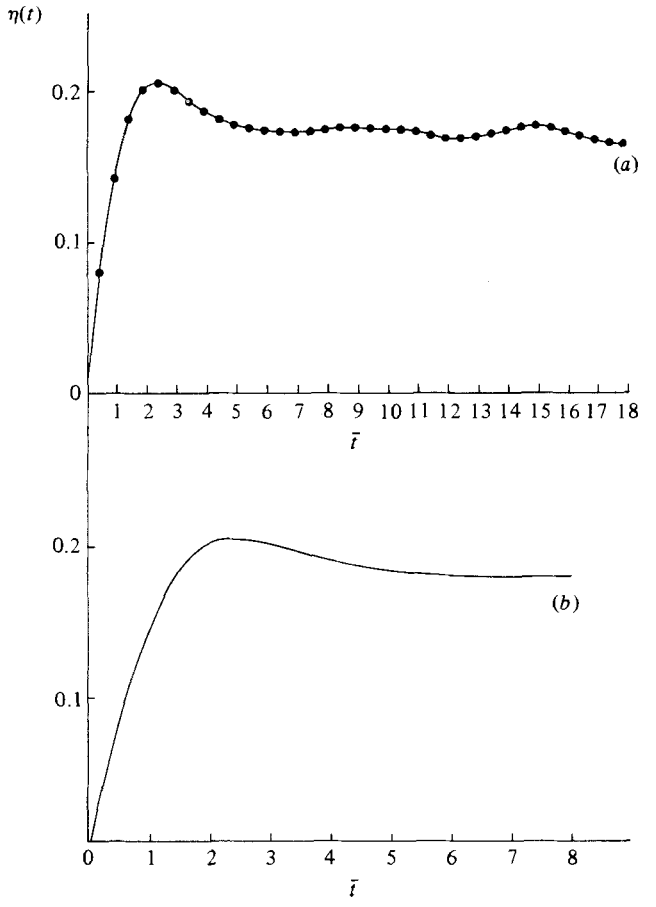

FIGURE 4. The eddy diffusivity $\eta(t) = \frac{1}{3}\langle \boldsymbol{x}(t)\cdot\boldsymbol{u}(\boldsymbol{x}(t),t)\rangle$ plotted against $t \equiv k_0 t$: (*a*) $k_0 = 6$, $\omega_0 = 0.1$, $\psi = 0$, $\kappa = 0$; (*b*) 6, 1, 0, 0.

consistent with those of Kraichnan. Moreover, because of the power of the DAP to produce large statistics we were able to follow the particle motion for larger times than Kraichnan. In some instances for over $70t_0$, where t_0 is characteristic of the time taken by the particle to travel one velocity-field correlation length and is given by $t_0^{-1} = u_0 k_0$.

In the absence of molecular diffusivity we can define an instantaneous effective diffusivity $\eta(t)$ by

$$\eta(t) = \tfrac{1}{3}\langle \boldsymbol{x}(t)\cdot\boldsymbol{u}(\boldsymbol{x}(t),t)\rangle. \tag{6.1}$$

We show the behaviour of $\eta(t)$ for two particular cases in figure 4. The value of $\eta(t)$ rises from zero, and after a few correlation times t_0 settles down to a fixed value, which it then maintains within statistical errors. These values are to be compared with the measured values of $\frac{1}{6}\mathrm{d}\langle \boldsymbol{x}^2(t)\rangle/\mathrm{d}t$. In our simulation the agreement between these two sets of values is extremely good (as it should be): the ratio is consistent with unity within errors. These results justify the confidence we place in our numerical procedures.

Our aim is to compare the simulation with an appropriate theoretical calculation. A relatively simple scheme is the self-consistent perturbation theory proposed by Phythian & Curtis (1978). In fact these authors demonstrated that their calculation

for the effective diffusivity was likely to be consistent with the results of Kraichnan (1970, 1976, 1977).

There were two barriers to a detailed comparison between the theoretical results and Kraichnan's simulation. The first was that for reasons of analytic simplicity Phythian & Curtis assumed a time dependence for the correlation functions of the form $e^{-\omega_0|t-t'|}$ rather than the Gaussian exponential $e^{-\frac{1}{2}\omega_0^2(t-t')^2}$ used by Kraichnan and ourselves. We have accordingly calculated in the Phythian & Curtis scheme but using the Gaussian time dependence. The second barrier was that Kraichnan's simulation did not contain the effects of molecular diffusivity. One of the attractions of the self-consistent perturbation theory is the very simple way in which the molecular diffusivity enters into the calculation. We have included the molecular diffusivity in our simulation using the techniques explained in §3.

In the perturbation-theory calculation the effective diffusivity η at long times is obtained as the solution of an equation of the form:

$$\eta-\kappa = F(\eta), \tag{6.2}$$

where $F(\eta)$ is obtained as a formal power series in u_0^2, and κ is the molecular diffusivity. $F(\eta)$ depends on the parameters of the velocity ensemble but not on κ. Using the correlation functions defined by (2.7)–(2.11), we have

$$F(\eta) = F_1(\eta)+F_2(\eta)+O(u_0^6), \tag{6.3}$$

where

$$F_1(\eta) = \tfrac{1}{3}u_0^2\int_0^\infty \mathrm{d}\tau \exp\{-\tfrac{1}{2}\omega_0^2\tau^2-\tau\eta k_0^2\}, \tag{6.4}$$

$$\begin{aligned} F_2(\eta) = &-\tfrac{1}{6}u_0^4k_0^2\int_0^\infty \mathrm{d}\tau\,\tau\int_0^\infty \mathrm{d}\tau' f(2\eta k_0^2\tau')\exp\{-\tfrac{1}{2}\omega_0^2(\tau+\tau')^2-\tfrac{1}{2}\omega_0^2\tau'^2-\eta k_0^2\tau\} \\ &-\tfrac{1}{12}u_0^4k_0^2\int_0^\infty \mathrm{d}\tau\int_0^\infty \mathrm{d}\tau'\int_0^\infty \mathrm{d}\tau''[g(2\eta k_0^2\tau')-\sin^2 2\psi f(2\eta k_0^2\tau')] \\ &\times\exp\{-\tfrac{1}{2}\omega_0^2(\tau+\tau')^2-\tfrac{1}{2}\omega_0^2(\tau'+\tau'')^2-\eta k_0^2(\tau+\tau'')\} \\ &+\tfrac{1}{9}u_0^4k_0^2\Big(\int_0^\infty \mathrm{d}\tau\exp\{-\tfrac{1}{2}\omega_0^2\tau^2-\eta k_0^2\tau\}\Big)^2. \end{aligned} \tag{6.5}$$

The functions $f(x)$ and $g(x)$ are defined by

$$\left.\begin{aligned} f(x) &= \frac{1}{2}\int_{-1}^{1}\mathrm{d}z\,(1-z^2)\,\mathrm{e}^{-x(1-z)}, \\ g(x) &= \frac{1}{2}\int_{-1}^{1}\mathrm{d}z\,z(1-z^2)\,\mathrm{e}^{-x(1-z)}. \end{aligned}\right\} \tag{6.6}$$

Note the presence of the helicity parameter ψ in (6.5), which allows us to obtain a theoretical prediction for the helicity dependence of the effective diffusivity. Our ability to adjust the helicity parameter in our velocity ensemble is a further advantage of our simulation and provides some of the most significant information contained in our results.

In comparing the theory with the simulation it is necessary to consider the cases of zero and non-zero helicity separately. For zero helicity and certain values of the other parameters, we show in figure 5 the graphs $y = F_1(\eta)$ and $y = F_1(\eta)+F_2(\eta)$. Curve (*b*) of figure 5 already well represents the frozen-turbulence limit $\omega_0\to 0$. The effective diffusivity is obtained to first and second order respectively by finding the points at

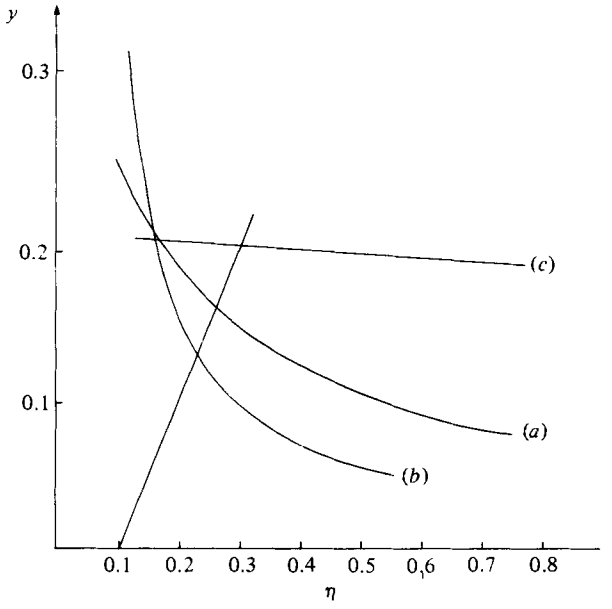

FIGURE 5. The curves $y = F(\eta)$ derived from self-consistent perturbation theory. The predicted effective difussivity is given by $\eta - \kappa = F(\eta)$, where κ is the molecular diffusivity. (*a*) $k_0 = 6$, $\omega_0 = 1$, $\psi = 0$; first-order estimate $y = F_1(\eta)$ defined in (6.4). (*b*) Parameters as in (*a*): second-order estimate $y = F_1(\eta) + F_2(\eta)$ defined in (6.4) and (6.5). (*c*) $k_0 = 1$, $\omega = 6$, $\psi = 0$; second-order estimate.

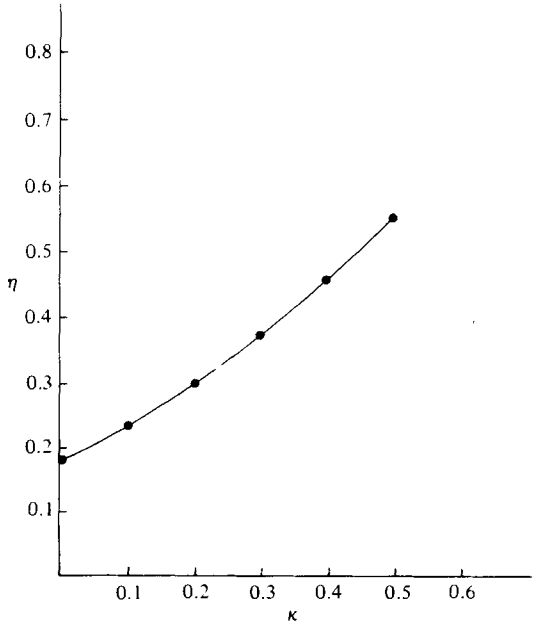

FIGURE 6. The theoretical curve of $\eta(\kappa)$ for $k_0 = 6$, $\omega_0 = 1$, $\psi = 0$ with the points (●) measured from the simulation. Numerical errors are smaller than the size of the data points.

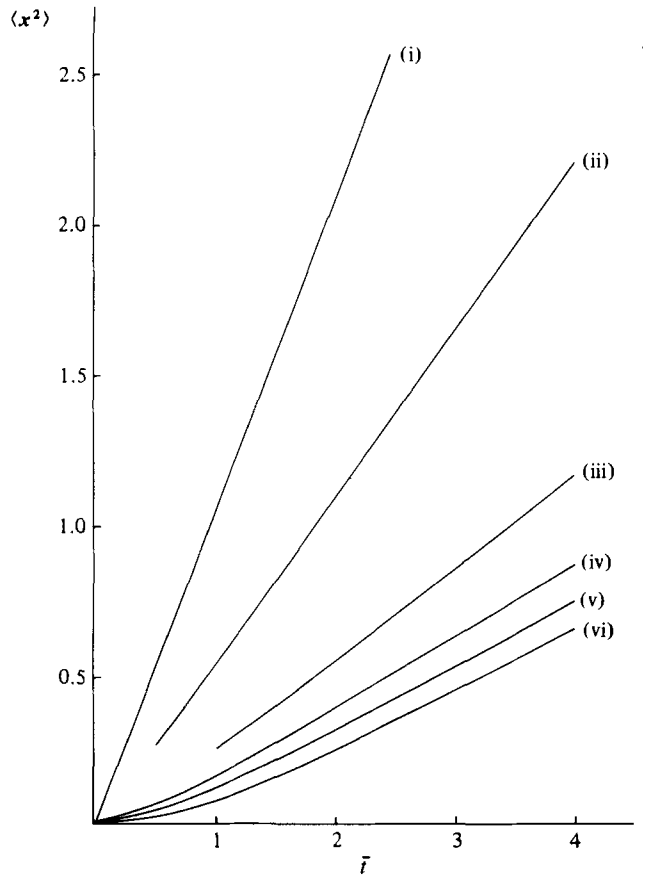

FIGURE 7. A plot of $\langle \boldsymbol{x}^2(t) \rangle$ versus $\bar{t} = k_0 t$ for $k_0 = 6$, $\omega_0 = 1$, $\psi = 0$ and various values of κ: (i) 1; (ii) 0.5; (iii) 0.2; (iv) 0.1; (v) 0.05; (vi) 0.

which these curves intersect the line $y = \eta - \kappa$. The resulting predictions for $\eta(\kappa)$ are shown in figure 6. The black circles represent the experimental points from the simulation measured by

$$\eta(\kappa) = \frac{1}{6}\frac{\mathrm{d}}{\mathrm{d}t}\langle \boldsymbol{x}^2(t) \rangle. \tag{6.7}$$

The size of the circles much exceeds the statistical error. A plot of $\langle \boldsymbol{x}^2(t) \rangle$ for various values of κ is shown in figure 7. Clearly the theoretical calculation to second order reproduces the results of the simulation with complete accuracy all the way from zero molecular diffusivity up to relatively large values. As a check on the perturbation series we have computed the third-order term in the series for $F(\eta)$ and we find that it is of negligible size, thus leaving the second-order (or two-loop) results unchanged.

It is reasonable to conclude that the self-consistent perturbation theory of Phythian & Curtis is both highly convergent and very accurate in predicting the effective diffusivity of Gaussian turbulence. Further confirmation of this conclusion is to be found in table 1, where we exhibit a comparison between the simulation and theory for different choices of parameters ranging from frozen turbulence ($u_0 k_0/\omega_0 \sim 10^7$) to the near-Markovian limit ($u_0 k_0/\omega_0 \sim 0.3$).

The real surprise in our results is the discrepancy that develops between the simulation and theory when the helicity parameter is increased from zero up to its

k_0	ω_0	κ	η (simulated)	η (theory)
6	10^{-6}	0	0.172 ± 0.003	0.176
6	0.1	0	0.172 ± 0.003	0.176
6	1	0	0.179 ± 0.001	0.18
6	1	0.1	0.238 ± 0.002	0.232
6	1	0.3	0.370 ± 0.004	0.371
6	1	0.4	0.452 ± 0.006	0.460
3	1	0	0.376 ± 0.005	0.36
1	3	0	0.401 ± 0.007	0.40
1	6	0	0.200 ± 0.007	0.207
1	6	0.1	0.298 ± 0.007	0.305
1	6	0.2	0.396 ± 0.007	0.400
1	6	0.5	0.691 ± 0.012	0.694

TABLE 1. A comparison for a number of cases of the effective diffusivity η predicted by self-consistent perturbation theory with the measured value for the simulation, $\eta = \frac{1}{6}(\langle \boldsymbol{x}^2(t+T) \rangle - \langle \boldsymbol{x}^2(t) \rangle)/T$

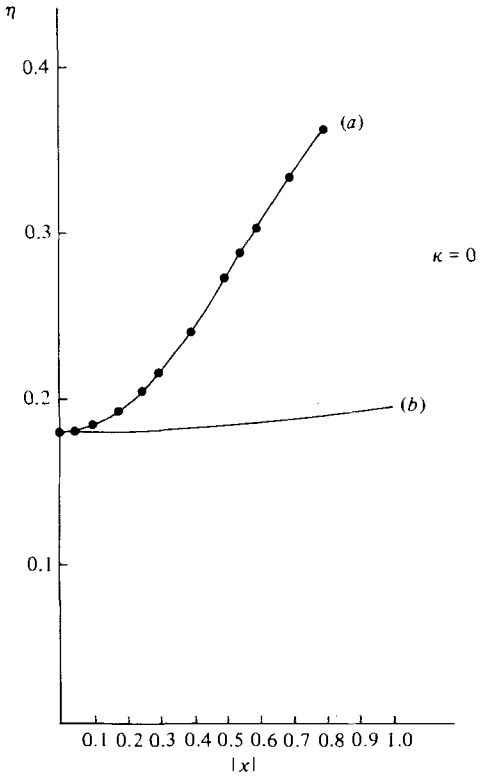

FIGURE 8. A plot of the effective diffusivity $\eta(x)$, where $x = \sin 2\psi$ for $k_0 = 6$, $\omega = 1$, $\kappa = 0$. (*a*) $\eta(x)$ measured in the simulation. (*b*) $\eta(x)$ predicted by third-order self-consistent perturbation theory. The errors on curve (*a*) are smaller than the data points.

maximum value. Figure 8 exhibits a typical case. According to the simulation the effective diffusivity increases by about 100% when the helicity is increased to near its maximum value. In contrast the theoretical prediction is scarcely influenced by the presence of helicity, as is also shown in figure 8. The corrections to theory from the third-order terms in the perturbation expansion have been calculated and are negligibly small for all values of the helicity.

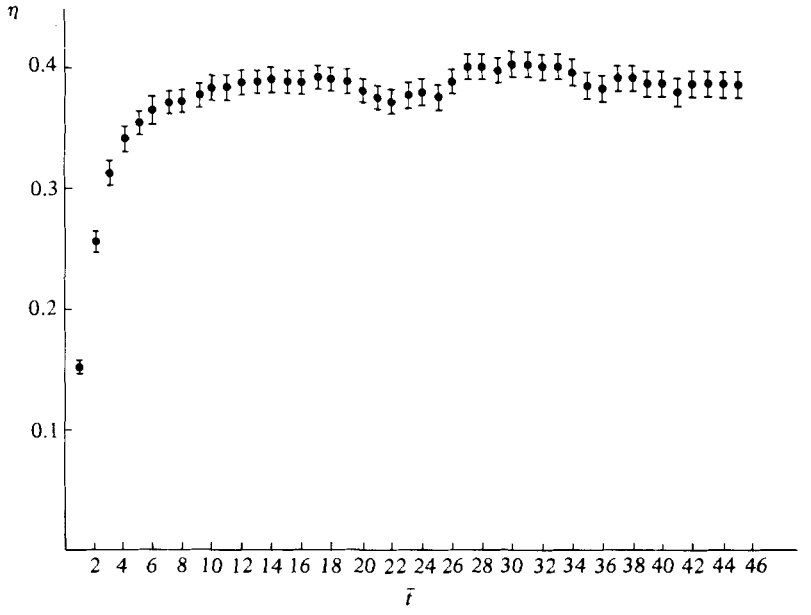

FIGURE 9. A point of $\eta(t) \equiv \frac{1}{6}\mathrm{d}\langle \boldsymbol{x}^2(t)\rangle/\mathrm{d}t$ versus $\bar{t} \equiv k_0 t$ for $k_0 = 6$, $\omega_0 = 1$, $\sin^2 2\psi = 0.9$, $\kappa = 0$.

We have demonstrated that the results of the simulation are correct and believable. First we showed in §5 that the short-time behaviour is correct for all values of the helicity, and secondly our results are consistent with those of Kraichnan (1970, 1976, 1977), who also obtained a considerable enhancement of the effective diffusivity when considering the case of turbulence with maximum helicity. Also our results for the case of zero helicity agree very well with the results of perturbation theory and confirm its applicability in this case.

An interesting effect in the case of near-maximal helicity is shown in figure 9, where $\eta(t)$ ($\equiv \frac{1}{6}\mathrm{d}\langle \boldsymbol{x}^2(t)\rangle/\mathrm{d}t$) is plotted, in this case (with $\kappa = 0$) for very large times. As the helicity is increased, the asymptotic region where $\eta(t)$ is a constant takes longer and longer to set in. This effect seems to be governed by a timescale which is somewhat larger than the obvious timescales of the turbulence and which increases with the increase of helicity. The work of Kraichnan also shows something of this effect.

If these observations are accepted then the only conclusion is that when helicity is present in the turbulence there are important *non-perturbative* contributions to the effective diffusivity. We may then conjecture that the large timescale involved corresponds to the time required to tunnel through the barrier between the perturbative and non-perturbative regions. To study non-perturbative contributions it is appropriate to use a path-integral formulation of the problem (Drummond 1982), and this is being actively investigated.

7. Conclusion

We have shown how a Gaussian turbulent velocity field with variable helicity may be constructed. We have also presented a numerical algorithm by which the time evolution of a scalar field transported by the turbulence and subject to molecular diffusion may be simulated by computer. By choosing the initial scalar field to be $\delta^{(3)}(\boldsymbol{x})$ the quantities $\langle \boldsymbol{x}^2(t)\rangle$ and $\langle (\boldsymbol{x}^2(t))^2\rangle$ averaged over the field can be measured and compared with theoretical expectations. The simulation was performed on the

j	1	2	3
α_{3j}	0.24997509	0.37079137	0.37923354
β_{3j}	0.81410000	−0.08766369	0.57406991
α_{2j}	0.00733232	0.66311191	—
α_{1j}	0.66275881	—	—

TABLE 2

DAP at Queen Mary College, London. The number of statistics was large enough to give negligible measured errors on any of the measured quantities. The short-time behaviour of $\langle \boldsymbol{x}^2(t) \rangle$ and $\langle (\boldsymbol{x}^2(t))^2 \rangle$ was compared with theory for various values of helicity and the other parameters controlling the turbulence. The agreement between the simulation and theory was very good in all cases. For long times the effective diffusivity defined in (6.7) was measured and found to be time-independent at sufficiently large times. For zero helicity the measured effective diffusivity was compared with the prediction of a second-order perturbation calculation based on the method of Phythian & Curtis (1978). In this case agreement was again excellent, and it was shown that the third-order corrections to theory were indeed negligible. However, for finite helicity rising to near maximal values the simulation gave measured effective diffusivities which increased by 100 %. The perturbation-theory estimates were hardly changed by the inclusion of helicity and hence were in total disagreement with the simulation of these effects, which are believable since we have been completely successful in measuring the short-time behaviour and the long-time behaviour with zero helicity. Also similar effects were observed by Kraichnan (1976, 1977). We conjecture that *non-perturbative* contributions become sizable and important for non-zero helicity. We suspect that the increasing length of evolution time needed to reach the asymptotic region of time-independent effective diffusivity is associated with the presence of such contributions.

It is worth emphasizing that these conclusions have considerable significance for the corresponding process of magnetic diffusion in plasmas, since in that case the presence of helicity is vital to the characteristic phenomenon of magnetic-field generation (Steenbeck, Krause & Radler 1966; Moffatt 1979). It would not be going too far to suggest that perturbation theory may also be misleading for the turbulence problem itself, since the transport of vorticity is to some extent analogous to the evolution of the magnetic field.

Appendix

The Nth-order generalized Runge–Kutta schemes for simulating the diffusion of a particle in a velocity field is obtained by introducing a sequence of N points and times $(\boldsymbol{x}_0, \boldsymbol{x}_1, \ldots, \boldsymbol{x}_N)$ and $(t_0, t_1, \ldots, t_N)$, where $\boldsymbol{x}_0 \equiv x$, $t_0 \equiv t$, $\boldsymbol{x}_N \equiv \boldsymbol{x} + \Delta \boldsymbol{x}$ and $t_N \equiv t + \Delta t$. The intermediate points are given by

$$t_i = t + \gamma_i \Delta t, \quad \boldsymbol{x}_i = \boldsymbol{x}_0 + \sum_{j=1}^{i} (\alpha_{ij} \boldsymbol{\mu}_j + \beta_{ij} \boldsymbol{\varepsilon}_j), \quad \boldsymbol{\mu}_i = \boldsymbol{u}(\boldsymbol{x}_{i-1}, t_{i-1})\, \Delta t, \quad \boldsymbol{\varepsilon}_i = (2\kappa \Delta t)^{\frac{1}{2}} \boldsymbol{\eta}_i,$$

where $i = 1, 2, \ldots, N$, and $\boldsymbol{\eta}_i$ are a set of independent random variables with unit variance and zero mean.

Ideally the coefficients are chosen in such a way as to reduce the error in the simulated probability distribution to $O(\Delta t^{N+1})$. In fact this is only exactly possible

for the case $N = 2$. We use the scheme $N = 3$ since it is possible to find a set of parameters that minimizes the error at $O(\Delta t^3)$. The set of coefficients is given by the following relations:

$$\beta_{31} = \beta_{21} = \beta_{11}, \quad \beta_{32} = \beta_{22},$$

$$\gamma_1 = \beta_{31}^2, \quad \gamma_2 = \beta_{31}^2 + \beta_{32}^2, \quad \gamma_3 = 1,$$

and the numerical values in table 2.

REFERENCES

DRUMMOND, I. T. 1982 Path-integral methods for turbulent diffusion. *J. Fluid Mech.* **123**, 59.

DRUMMOND, I. T., DUANE, S. & HORGAN, R. R. 1983 The stochastic method for numerical simulations: higher order corrections. *Nucl. Phys.* **B220** [FS8], 119.

KRAICHNAN, R. H. 1970 Diffusion by a random velocity field. *Phys. Fluids* **13**, 22.

KRAICHNAN, R. H. 1976 Diffusion of passive scalar and magnetic fields by helical turbulence. *J. Fluid Mech.* **77**, 753.

KRAICHNAN, R. H. 1977 Lagrangian velocity covariance in helical turbulence. *J. Fluid Mech.* **81**, 385.

PHYTHIAN, R. & CURTIS, W. D. 1978 The effective long-time diffusivity for a passive scalar field in a Gaussian model flow. *J. Fluid Mech.* **89**, 241.

SAFFMAN, P. G. 1960 On the effect of molecular diffusivity in turbulent diffusion. *J. Fluid Mech.* **8**, 273.

MOFFATT, H. K. 1979 *Magnetic Field Generation in Electrically Conducting Fluids.* Cambridge University Press.

STEENBECK, M., KRAUSE, F. & RADLER, K.-H. 1966 *Z. Naturforsch.* **21a**, 369.